## Title

The Design and Manufacture of a Gear-Coupled Serial Chain to Trace the Butterfly Curve



## ISBN

978-0-7918-5817-2

## Authors

Liu, Yang
Wang, Peter Lee-Shien
McCarthy, J Michael

## Publication Date

2017-08-06

## DOI

10.1115/detc2017-68388

**Proceedings of the ASME 2017 International Design Engineering Technical Conferences and Computers and Information in Engineering Conference**
**IDETC/CIE 2017**
**August 6-9, 2017, Cleveland, Ohio, USA**

**DETC2017-68388**

# THE DESIGN AND MANUFACTURE OF A GEAR-COUPLED SERIAL CHAIN TO TRACE THE BUTTERFLY CURVE

**Yang Liu***
Robotics and Automation Laboratory
Department of Mechanical
and Aerospace Engineering
University of California
Irvine, California 92697
Email: liuy14@uci.edu

**Peter Lee-Shien Wang**
Robotics and Automation Laboratory
Department of Mechanical
and Aerospace Engineering
University of California
Irvine, California 92697
Email: wangpl1@uci.edu

**J. Michael McCarthy**
Robotics and Automation Laboratory
Department of Mechanical
and Aerospace Engineering
University of California
Irvine, California 92697
Email: jmmccart@uci.edu

## ABSTRACT

*This paper presents a design and manufacturing methodology for a mechanical system that draws trigonometric curves assembled from a series of links connected by gears. We demonstrate this technique using 11 gear-coupled links that trace a butterfly curve. The equation of a butterfly curve is converted to the relative rotations of the links of a coupled serial chain assembled so it operates with one input. We present a procedure to determine the adjustments to the gear ratios and link dimensions necessary for practical manufacture of the mechanism. The results are demonstrated by a working prototype.*

## INTRODUCTION

This paper presents the details necessary to manufacture the system formed by a gear-coupled serial chain that traces a complex plane curve such as the "Butterfly curve" [1]. The result is a coupled serial chain where the sequence of links are connected by cable, belt or gear drive [2]. Our goal is to present the adjustments necessary to use additive manufacturing for the design of this complex mechanism. The result is a system that uses a total of 32 gears with custom gear ratios. The link geometries were developed to reduce weight and increase cross-sectional moment of inertia. Finally, a combination of acetone and a silicon lubricant were used to perform the final fitting of the revolute joints to obtain a tight clearance with minimal friction.

## LITERATURE REVIEW

Krovi et al. [2, 3] provide a design methodology for single degree of freedom linkage systems formed as serial chains with joints coupled by belt and cable drives. Recent work by Liu and McCarthy [4] shows the usage of belt and cable drives to design mechanisms to trace plane algebraic curves. The use of belt and cable drives to actuate the joints of robotic hands can be found in [5–7]. Collins [8] uses a combination of cables and gears to actuate finger joints, while Lin [9] uses gears. Our approach follows Krovi, but uses gearing to provide the joint coupling.

The use of additive manufacturing for the fabrication of mechanical systems can be traced to Mavroidis [10] and Laliberte [11]. The manufacturing options include selective laser melting [12], stereolithography and selective laser sintering [13], and layer building technology [14]. Research in additive manufacturing of mechanisms generally focuses on techniques to avoid assembly [15]. In this paper, we use fused deposition modeling by the Stratasys Fortus 450mc, which requires manufacture of individual components and assembly to maintain tolerances, but is fast and inexpensive for prototype development [16].

*Address all correspondence to this author.

 

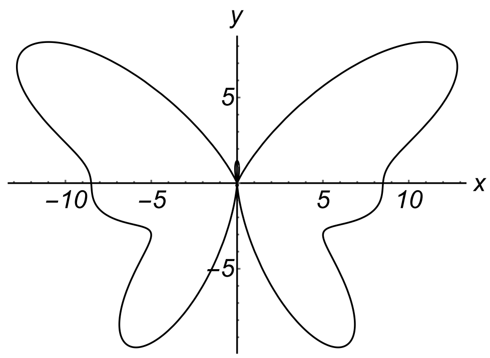


**FIGURE 1**. A plot of a butterfly curve of dimension ±12 cm wide

## PRELIMINARIES

Liu and McCarthy [1] have shown that a trigonometric plane curve, $\mathbf{P} = (x(\theta), y(\theta))$,

$$P = \begin{Bmatrix} x(\theta) \\ y(\theta) \end{Bmatrix} = \begin{Bmatrix} \sum_{k=0}^{m} a_k \cos k\theta + b_k \sin k\theta \\ \sum_{k=0}^{m} c_k \cos k\theta + d_k \sin k\theta \end{Bmatrix}, \quad (1)$$

where $a_k$, $b_k$, $c_k$ and $d_k$, $k = 0, \ldots, m$, are real coefficients and $\theta \in [0, 2\pi]$, can be converted to the form,

$$P(\theta) = \begin{Bmatrix} \sum_{k=0}^{m} L_k \cos(k\theta - \psi_k) + M_k \cos(-k\theta - \eta_k) \\ \sum_{k=0}^{m} L_k \sin(k\theta - \psi_k) + M_k \sin(-k\theta - \eta_k) \end{Bmatrix}, \quad (2)$$

in which,

$$\begin{aligned} L_k &= \frac{1}{2}\sqrt{(a_k + d_k)^2 + (c_k - b_k)^2}, \\ M_k &= \frac{1}{2}\sqrt{(a_k - d_k)^2 + (c_k + b_k)^2}, \end{aligned} \quad (3)$$

and

$$\psi_k = \arctan \frac{c_k - b_k}{a_k + d_k}, \quad \eta_k = \arctan \frac{c_k + b_k}{a_k - d_k}. \quad (4)$$

The result is an equation that can be interpreted as a sequence of links driven at a prescribed set of speed ratios $k = 1, \ldots, m$ to trace the curve. Equation 3 defines the lengths of the links $L_k$ and $M_k$ and (4) defines the phase angles $\psi_k$ and $\eta_k$ of their movement.

## BUTTERFLY CURVE

When the equation of the Butterly curve [17],

$$\begin{aligned} P_B:\ \rho(\theta) =& 7 - \sin\theta + 2.3\sin 3\theta + 2.5\sin 5\theta - 2\sin 7\theta \\ & - 0.4\sin 9\theta + 4\cos 2\theta - 2.5\cos 4\theta, \end{aligned} \quad (5)$$

is written in the form of (2), we obtain the link lengths and phase angles listed in Table 1. The $k = 0$ row defines the ground pivot position. There are totally 14 links consisting the coupled serial chain to generate the butterfly curve shown in Figure 1.

**TABLE 1**. Speed ratios, link length ratios and phase angles for the butterfly curve

| k | $L_k$ | $\psi_k$ | $M_k$ | $\eta_k$ |
|---|---|---|---|---|
| 0 | 0.25 | $-\pi/2$ | 0.25 | $-\pi/2$ |
| 1 | 7 | 0 | 2 | 0 |
| 2 | 0.5 | $\pi/2$ | 1.15 | $\pi/2$ |
| 3 | 2 | 0 | 1.25 | $\pi$ |
| 4 | 1.15 | $-\pi/2$ | 1.25 | $\pi/2$ |
| 5 | 1.25 | $\pi$ | 0 | 0 |
| 6 | 1.25 | $-\pi/2$ | 1 | $-\pi/2$ |
| 7 | 0 | 0 | 0 | 0 |
| 8 | 1 | $\pi/2$ | 0.2 | $-\pi/2$ |
| 9 | 0 | 0 | 0 | 0 |
| 10 | 0.2 | $\pi/2$ | 0 | 0 |

This is the starting point for the design of our mechanism. In what follows, we adjust these dimensions to facilitate manufacture using Additive Manufacturing.

## DESIGN MODIFICATIONS

The build envelope of the Stratasys Fortus 450mc additive manufacturing system is $406 \times 355 \times 406$ mm, which sets a limit to the size of our mechanism. Our experiments showed that the smallest feature size that we could reliably generate was a 10mm hole for the link joints. This restricted the size of our gears to a minimum diameter of 15mm, which in turn sets our minimum link dimension to be 20mm.

If the dimension of the smallest link in Table 1 to be 20mm, the longest link must be 700mm, which is beyond the build envelop of the Stratasys Fortus printer. If we eliminate the three shortest links, we can reduce the size of the largest link to 210mm. Specifically, we delete the links denoted as $L_2$, $L_{10}$ and $M_8$. The resulting Butterfly curve differs from the original curve by a maximum of 21.6mm, see Figure 2. The dimensions for manufacturing prototype are listed in Table 2. This removes the high frequency terms, which reduces the curvature and softens the curve.

 

**TABLE 2**. Speed ratios, link length ratios and phase angles for the manufacturing prototype

| k | $L_k$ | $\psi_k$ | $M_k$ | $\eta_k$ |
|---|---|---|---|---|
| 0 | 0.25 | $-\pi/2$ | 0.25 | $-\pi/2$ |
| 1 | 7 | 0 | 2 | 0 |
| 2 | 0 | 0 | 1.15 | $\pi/2$ |
| 3 | 2 | 0 | 1.25 | $\pi$ |
| 4 | 1.15 | $-\pi/2$ | 1.25 | $\pi/2$ |
| 5 | 1.25 | $\pi$ | 0 | 0 |
| 6 | 1.25 | $-\pi/2$ | 1 | $-\pi/2$ |
| 7 | 0 | 0 | 0 | 0 |
| 8 | 1 | $\pi/2$ | 0 | 0 |
| 9 | 0 | 0 | 0 | 0 |
| 10 | 0 | 0 | 0 | 0 |

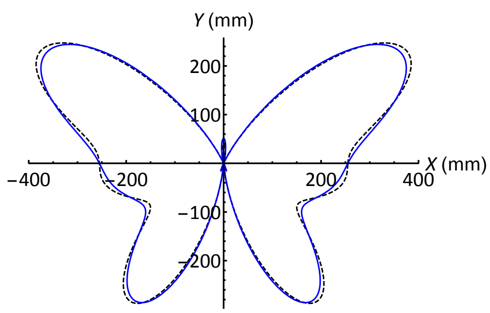


**FIGURE 2**. The Butterfly mechanism is to draw a curve $\pm 40$ cm wide (solid line). Using 11 links in the coupled serial chain introduces variations from the original 14 link version (dashed line)

## DRIVE TRAIN

The drawing mechanism for trigonometric curves uses pairs of links that rotate in opposite directions [1]. The speed ratio for each link in the chain is given by $+k$ for links $L_k$ and $-k$ for links $M_k$. This speed ratio is measured relative to the world frame. By introducing relative speed ratios at each link, we can simplify the construction of the mechanism using gear trains.

The drawing mechanism consists of a sequence of joints $G_j$ and links $B_j$, $j = 1, \ldots, 11$ connected in series and attached by joint $G_1$ to a base, Figure 3. Each link $B_j$ has a gear fixed to the link and centered on its joint $G_j$, which for convenience we call $G_j$ as well. This joint includes a bearing that engages the axle mounted on the previous link $B_{j-1}$. The link $B_j$ has an axle at the end opposite to joint $G_j$ that engages the bearing of $G_{j+1}$ on link $B_{j+1}$.

Each joint $G_j$ includes a second gear $D_j$ that is rigidly mounted to the axle of previous link $B_{j-1}$. Similarly, the axle at the other end of link $B_j$ engages and is fixed to the gear $D_{j+1}$.

The drive system consists of a sequence of connections between gear $D_j$ and the gear $G_{j+1}$. To start, $D_1$ is rigidly mounted to an axle attached to the base, and the mechanism is actuated by a drive gear that engages $G_1$.

This configuration allows us to define the relative speed ratios between the gears $D_j$ and $G_{j+1}$ when the link $B_j$ is held fixed,

$$\frac{\omega_{j+1,j}}{\omega_{j-1,j}} = \frac{T_{D,j}}{T_{G,j+1}}, \tag{6}$$

where $T_{D,j}$ and $T_{G,j+1}$ are the teeth number of the gear $D_j$ and $G_{j+1}$.

The relative speed ratios are related to world frame speed ratios listed in Table 2, by

$$\omega_{j+1,j} = \omega_{j+1} - \omega_j, \tag{7}$$

therefore the relative speed ratio are given by,

$$\frac{\omega_{j+1,j}}{\omega_{j-1,j}} = \frac{\omega_{j+1} - \omega_j}{\omega_{j-1} - \omega_j}. \tag{8}$$

From these equations, we calculate the gears that provide the world frame speed ratios that we need.

Figure 3 shows the structure of a serial chain consisting of three links. The gear $D_1$ is rigidly attached to the base. Link $B_1$, $B_2$ and $B_3$ have gear $G_1$, $G_2$ and $G_3$ fixed to them respectively. The relative rotation is achieved by adding chain driven between gear $D_1$ and $G_2$, and between gear $D_2$ and $G_3$. The resulting mechanical system has a single degree of freedom.

In the chain driving configuration, we assume the links are lined up with one counter-clockwise rotating link followed by one clockwise rotating link. The world frame is built along the base. In the world frame, we denote the angular velocities of link $B_j$ and gear $G_j$ as $\omega_{Bj}$ and $\omega_{Gj}$, respectively. It is obvious that $\omega_{Bj} = \omega_{Gj}$. We use the denotation $\omega_{Dj}$ for the angular velocity of gear $D_j$. From Table 2, we have the speed ratios for all the links.

Figure 4 shows the angular velocities of the components that drive the first two links in the world frame. The gear $D_1$ is static relative to the world frame thus $\omega_{D1} = 0$. Reference frame 1 is built along link $B_1$. Figure 5 shows the angular velocities of the components in reference frame 1. We denote the teeth number of the gear $D_j$ and $G_j$ as $T_{D,j}$ and $T_{G,j}$, respectively. Thus we can calculate the ratio of the teeth number between gear $D_1$ and $G_2$ as

$$\frac{T_{D,1}}{T_{G,2}} = \frac{\omega'_{G2}}{\omega'_{D1}} = \frac{\omega_{B2} - \omega_{B1}}{-\omega_{B1}} \tag{9}$$

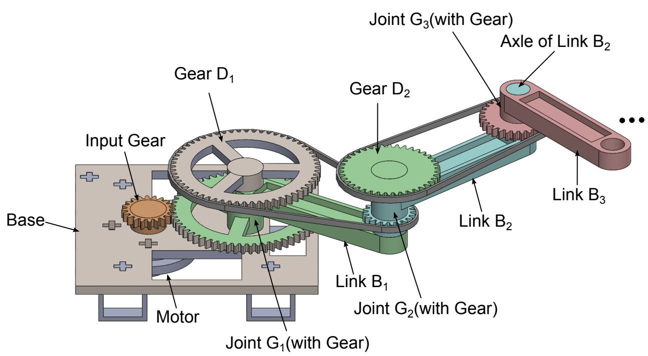


**FIGURE 3**. The structure of a coupled serial chain consisting of three links

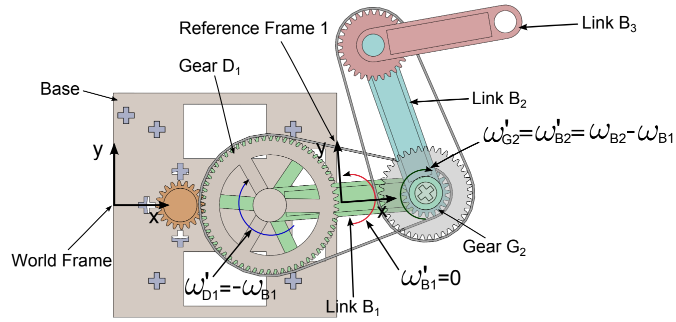


**FIGURE 5**. The angular velocities of the components for the first two links in the reference frame 1

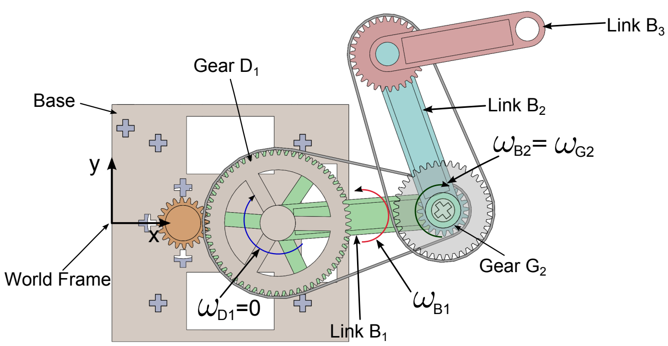


**FIGURE 4**. The angular velocities of the components for the first two links in the world frame

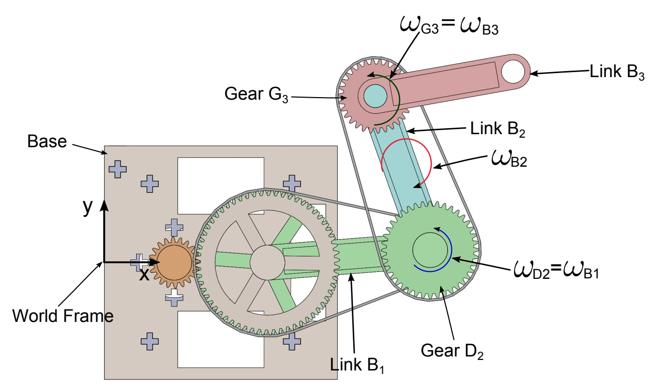


**FIGURE 6**. The angular velocities of the driving components from link $B_2$ to link $B_3$ in the world frame

Figure 6 and Figure 7 show the angular velocities of the driving components from link $B_2$ to link $B_3$ in the world frame and reference frame 2, respectively. Similarly, we can calculate the relative size of gear $D_2$ and $G_3$ as

$$\frac{T_{D,2}}{T_{G,3}} = \frac{\omega'_{G3}}{\omega'_{D2}} = \frac{\omega_{B3} - \omega_{B2}}{\omega_{B1} - \omega_{B2}} \tag{10}$$

Therefor the equation to calculate the relative size of gear $D_j$ with respect to gear $G_{j+1}$ can be obtained as

$$\frac{T_{D,j}}{T_{G,j+1}} = \frac{\omega'_{G(j+1)}}{\omega'_{Dj}} = \frac{\omega_{B(j+1)} - \omega_{B(j)}}{\omega_{B(j-1)} - \omega_{Bj}} \tag{11}$$

## THE COUPLED SERIAL CHAIN MECHANISM

In this section, we present the methodology of using relative rotation to build a coupled serial chain mechanism that can trace the butterfly curve showing in solid line in Figure 2. The resulting mechanism has a single degree of freedom. Recall that we have eleven links in our manufacturing version of coupled serial chain. The column $k$ in Table 2 defines the speed ratios for all the

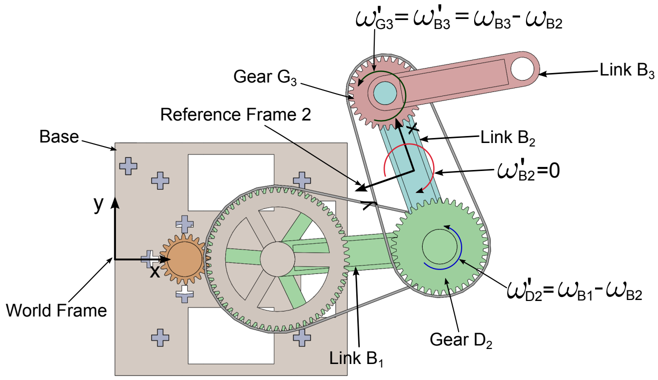


**FIGURE 7**. The angular velocities of the driving components from link $B_2$ to link $B_3$ in the reference frame 2

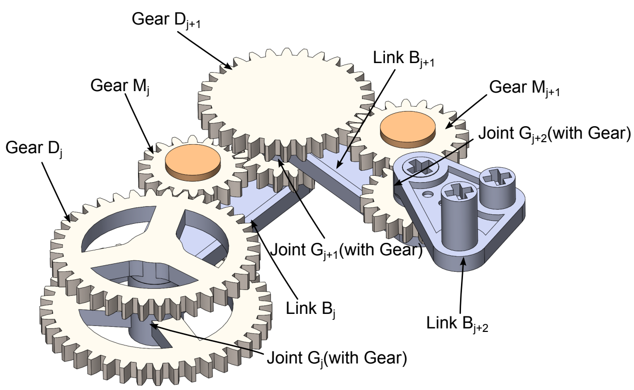


**FIGURE 8**. The configuration of gear driving from Link $B_j$ to Link $B_{j+2}$

links. The ground pivot position is given by the $k = 0$ row in Table 2. We have six links that rotate counter-clockwise are $L_1$, $L_3$, $L_4$, $L_5$, $L_6$ and $L_8$, and another set of five links rotate clockwise are $M_1$, $M_2$, $M_3$, $M_4$ and $M_6$. In our configuration, we line up all the links from the longest to the shortest according to their length $S_j$. Additionally, the links are assembled in a way such that the counter-clockwise rotating links are followed by a clockwise rotating link and vice versa. Therefore, the sequence of the eleven links in the serial chain is $L_1$, $M_1$, $L_3$, $M_3$, $L_5$, $M_4$, $L_6$, $M_2$, $L_4$, $M_6$ and $L_8$. The links in this sequence are denoted as $B_j$ ($j = 1 \cdots 11$) and the associated phase angle for each link is denoted as $\delta_j$.

Rather than a chain driven, we introduce an alternative method of driving the mechanism to include a middle gear $M_j$

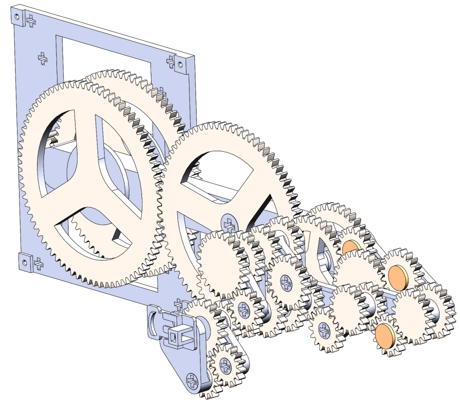

**FIGURE 9**. The solid model of the Butterfly mechanism to be built using additive manufacturing

between gear $D_j$ and $G_{j+1}$. We replace the links with plates and locate the middle gear $M_j$ a position such that its pitch circle is tangent to the pitch circles of both the gear $D_j$ and $G_{j+1}$. Figure 8 shows the configuration the components from link $B_j$ to link $B_{j+2}$. Note that in order to keep the relative rotation speed, the middle gear $M_j$ has to be the same size as gear $D_j$ or the $G_{j+1}$. The teeth number of the gear $M_j$ is denoted as $T_{M,j}$.

By applying (11), we can obtain the relative size of the gear $D_j$ and $G_{j+1}$. We make the module of all the gears to be $m$. The addendum of the gear is denoted as $a$. In order to make the three gears assembled on each plate mesh correctly, the following two conditions must be satisfied, such that

$$\frac{m}{2}(T_{D,j} + T_{G,j+1}) + 2a < S_k \tag{12}$$

$$\begin{aligned} \frac{m}{2}(3T_{D,j} + T_{G,j+1}) \geq S_k \quad or \\ \frac{m}{2}(T_{D,j} + 3T_{G,j+1}) \geq S_k \end{aligned} \tag{13}$$

Equation 12 makes sure the gear $D_j$ and $G_{j+1}$ do not conflict with each other. Equation 13 guarantees that the gear $D_j$, $M_j$ and $G_{j+1}$ are close enough to mesh with each other correctly. In our model, we choose the gear module $m = 1.5$ and addendum $a = 1.5$mm. We make the length of the smallest link to be 30mm. The dimensions for all the components are listed in Table 3. The manufacturing model of our linkage is shown in Figure 9. The simulation of the motion of our mechanism is shown in Figure 10.

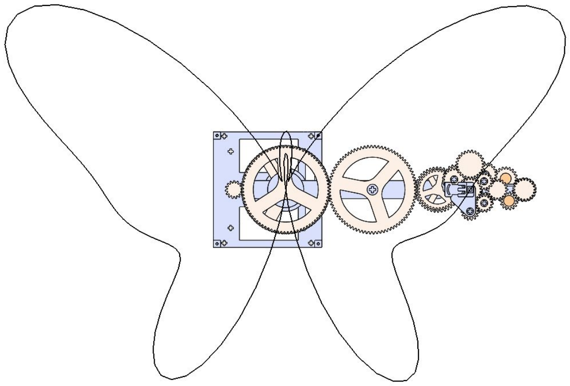

**FIGURE 10**. Simulation of the end-effector movement of the Butterfly mechanism using *SolidWorks Motion Analysis*

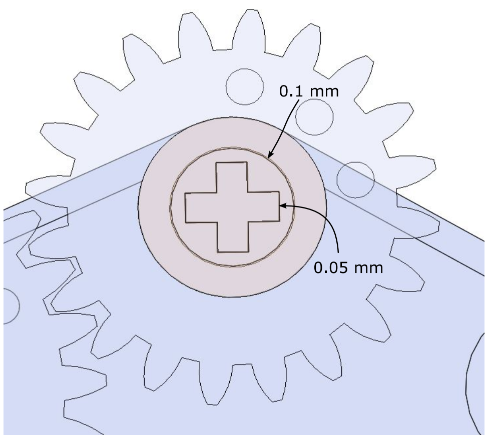


**FIGURE 11**. Dimensional differences for mounting features for gear and link axle are specified to be less than the resolution of the Fortus 450mc system. The parts are manually fit to ensure performance

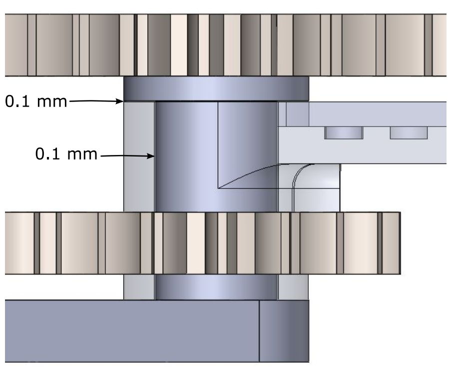


**FIGURE 12**. Dimensional differences between assembly features is less than the resolution of the Fortus 450mc system, therefore manual fit is required

**TABLE 3**. Manufacturing dimensions of the single coupled serial chain to draw the butterfly curve

| j | k | $B_j$ | $S_j$ | $\delta_j$ | $T_{D,j}$ | $T_{M,j}$ | $T_{G,j+1}$ |
|---|---|---|---|---|---|---|---|
| 1 | 1 | $L_1$ | 210 | 0 | 80 | 80 | 40 |
| 2 | -1 | $M_1$ | 60 | 0 | 36 | 18 | 18 |
| 3 | 3 | $L_3$ | 60 | 0 | 30 | 20 | 20 |
| 4 | -3 | $M_3$ | 37.5 | $\pi$ | 20 | 15 | 15 |
| 5 | 5 | $L_5$ | 37.5 | $\pi$ | 18 | 16 | 16 |
| 6 | -4 | $M_4$ | 37.5 | $\pi/2$ | 20 | 18 | 18 |
| 7 | 6 | $L_6$ | 37.5 | $-\pi/2$ | 16 | 20 | 20 |
| 8 | -2 | $M_2$ | 34.5 | $\pi/2$ | 15 | 20 | 20 |
| 9 | 4 | $L_4$ | 34.5 | $-\pi/2$ | 25 | 15 | 15 |
| 10 | -6 | $M_6$ | 30 | $-\pi/2$ | 21 | 15 | 15 |
| 11 | 8 | $L_8$ | 30 | $\pi/2$ | 0 | 0 | 0 |

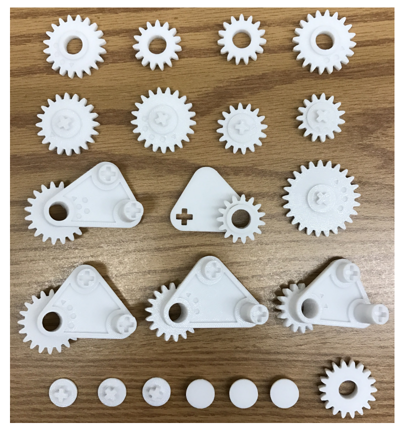

**FIGURE 13**. Example of the Butterfly mechanism drive components manufactured by the Fortus 450mc system.

## PHYSICAL PROTOTYPE

We used the Stratsys Fortus 450mc additive manufacturing system to build all the components for our linkage. These include 11 links, 32 gears, ground pivot and the input crank. The resolution of the Stratsys printer is 0.127 mm. Through repeated experimentation, we sized the clearance between the revolute joint and the pivot to be 0.1 mm. An acetone and silicon combination solution was used to simultaneously wear the size of joint pin and hole to a tight tolerance while lubricating the contact surface to minimize friction. In order to ensure the cap gear tightly assembled to the link joint, the clearance fitting was tested and determined to be 0.05 mm. The clearance between components is shown in Figure 11 and Figure 12.

We manufactured all the components individually and assembled them together to obtain our serial coupled serial chain

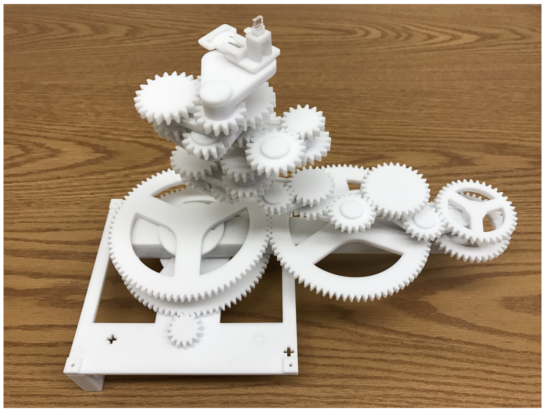

**FIGURE 14**. The fully assembled Butterfly mechanism

that can trace the butterfly curve. Part of the components are shown in Figure 13. The final manufactured prototype is shown in Figure 14.

## CONCLUSION

This paper presents the manufacturing details for the construction of complex systems to draw trigonometric curves using additive manufacturing. The method is demonstrated for the 14 link Butterfly curve, which must simplified to an 11 link system to fit the requirements of the Stratasys Fortus system. We show how to adjust the dimensions of the gears to accomplish the desired joint movement within the tolerances available to this manufacturing process. The result is a functional prototype butterfly linkage drawing mechanism. Future work will simplify design and improve the manufacturing quality of these systems.

## REFERENCES


[1] Liu, Y., and McCarthy, J. M., 2017. "Design of mechanisms to draw trigonometric plane curves". *In Press Journal of Mechanisms and Robotics, doi: 10.1115/1.4035882*.

[2] Nie, X., and Krovi, V., 2005. "Fourier methods for kinematic synthesis of coupled serial chain mechanisms". *Journal of Mechanical Design*, ***127***, pp. 232–241.

[3] Krovi, V., Ananthasuresh, G., and Kumar, V., 2002. "Kinematic and kinetostatic synthesis of planar coupled serial chain mechanisms". *TRANSACTIONS-AMERICAN SOCIETY OF MECHANICAL ENGINEERS JOURNAL OF MECHANICAL DESIGN*, ***124***(2), pp. 301–312.

[4] Liu, Y., and McCarthy, J. M., 2017. "Synthesis of a linkage to draw a plane algebraic curve". *Mechanism and Machine Theory*, ***111***(5), pp. 10–20.

[5] Leaver, S., McCarthy, J. M., and Bobrow, J. E., 1988. "The design and control of a robot finger for tactile sensing". *Journal of Field Robotics*, ***5***(6), pp. 567–581.

[6] Jacobsen, S. C., Ko, H., Iversen, E. K., and Davis, C. C., 1989. "Antagonistic control of a tendon driven manipulator". In Robotics and Automation, 1989. Proceedings., 1989 IEEE International Conference on, IEEE, pp. 1334–1339.

[7] Yang, Y., Zhang, W., Xu, X., Hu, H., and Hu, J., 2017. "Lipsa hand: A novel underactuated hand with linearly parallel and self-adaptive grasp". In Mechanism and Machine Science: Proceedings of ASIAN MMS 2016 & CCMMS 2016, Springer, pp. 111–119.

[8] Collins, C. L., 2003. "Kinematics of robot fingers with circular rolling contact joints". *Journal of Field Robotics*, ***20***(6), pp. 285–296.

[9] Lin, L.-R., and Huang, H.-P., 1996. "Mechanism design of a new multifingered robot hand". In Robotics and Automation, 1996. Proceedings., 1996 IEEE International Conference on, Vol. 2, IEEE, pp. 1471–1476.

[10] Mavroidis, C., DeLaurentis, K. J., Won, J., and Alam, M., 2000. "Fabrication of non-assembly mechanisms and robotic systems using rapid prototyping". *Journal of Mechanical Design*, ***123***(4), pp. 516–524.

[11] Laliberte, T., Gosselin, C., and Cote, G., 1999. "Rapid prototyping of mechanisms". In Proceedings of the 10th World Congress on the Theory of Machines and Mechanisms, Vol. 3, pp. 959–964.

[12] Yang, Y.-q., Su, X.-b., Wang, D., and Chen, Y.-h., 2011. "Rapid fabrication of metallic mechanism joints by selective laser melting". *Proceedings of the Institution of Mechanical Engineers, Part B: Journal of Engineering Manufacture*, ***225***(12), pp. 2249–2256.

[13] Calì, J., Calian, D. A., Amati, C., Kleinberger, R., Steed, A., Kautz, J., and Weyrich, T., 2012. "3d-printing of non-assembly, articulated models". *ACM Transactions on Graphics (TOG)*, ***31***(6), p. 130.

[14] Chen, Y., and Zhezheng, C., 2011. "Joint analysis in rapid fabrication of non-assembly mechanisms". *Rapid Prototyping Journal*, ***17***(6), pp. 408–417.

[15] De Laurentis, K. J., and Mavroidis, C., 2004. "Rapid fabrication of a non-assembly robotic hand with embedded components". *Assembly Automation*, ***24***(4), pp. 394–405.

[16] Rodriguez, F., and Tovar, A., 2008. "Coupler-based synthesis of a rssr mechanism". In EngOpt 2008 - International Conference on Engineering Optimization.

[17] Fay, T. H., 1989. "The butterfly curve". *Amer. Math. Monthly*, ***96***, pp. 442–443.